Paper presented at Dynamics and Control of Systems and Structures in Space (DCSSS),
5th conference, Kings College, Cambridge, July 2002

Evaluation of the SPH Method for the Modelling of Spall in Anisotropic Alloys

Tom De Vuyst[a], Rade Vignjevic[a], Neil K. Bourne[b], James Campbell[a]

[a]Structures and Materials Group, College of Aeronautics,
Cranfield University, Beds, MK43 0AL, UK,
[b]Royal Military College of Science,
Cranfield University, Shrivenham, SN6 8LA, UK

Abstract

Spall caused by hypervelocity impacts at the lower range of velocities could result in significant damage to spacecraft. A number of polycrystalline alloys, used in spacecraft manufacturing, exhibit a pronounced anisotropy in their mechanical properties. The aluminium alloy AA 7010, whose orthotropy is a consequence of the meso-scale phase distribution or grain morphology, has been chosen for this investigation. The material failure observed in plate impact was simulated using an explicit finite element code and a smoothed particle hydrodynamics (SPH) code. A number of spall models where used, and the Hugoniot Elastic Limit (HEL) and spall strength have been studied as a function of orientation, and compared to experimental results.

Introduction

The effect of orientation on the mechanical properties of metals and alloys is well known and has been studied extensively under quasi-static conditions. This can occur on three levels, these being at the unit cell, the microstructural level (due to preferred orientation of the grain structure) or the meso-scale due to either phase distribution or grain morphology. Smallman [9] gives a more complete discussion of such behaviour. In contrast, similar measurements made at dynamic strain-rates are not as extensive. Gray *et al* [2] investigated two types of zirconium, a cold-rolled one and annealed one. Peak stresses in the through-thickness direction were about 2.5 times greater when compared to the in-plane direction for the same plate for quasi-static loading regimes. In the case of shock loading, the variation of the Hugoniot Elastic Limit (HEL) was consistent with the quasi-static measurements. Orientation had a significant effect on damage evolution, but a minimal effect on the spall was observed in rear surface visar traces. Similar measurements have also been made on a eutectoid 1080 rail steel Gray *et al*. [3]. This material is crystallographically isotropic, but possesses microstructural anisotropy due to the presence of manganese sulphide (MnS) stringers that orientate themselves along the rolling direction. It exhibited a significantly lower spall strength when loaded transverse to the MnS stringers than when loaded in parallel to them.

The behaviour of aluminium alloys under shock loading has been studied in some depth by Ek *et al*. [1], Moshe *et al.* [6] and Zheng *et al.* [10]. Their low densities and (in some alloys at least) high strengths has motivated their use as light-weight armours and airframes. Possibly the most thorough study on a single alloy was made by Rosenberg *et al*. [7]. Here, they showed that in the alloy 2024 (Al+Cu+Mg), the HEL and spall strength followed the same trends as the quasi-statically measured yield strength, with the lowest measured in the solution-treated material. They also demonstrated that spall strength was affected by material orientation. In this case the lower spall strength was observed perpendicular to the rolling direction when compared to that measured parallel to it. In this paper, simulation results are presented for the alloy 7010-T6, a high-strength airframe alloy (Al+Zn+Mg+Cu), where the HEL and spall strength in the short transverse and longitudinal (rolling) directions were compared with experimental results by Millett *et al*. [5].

Experiment

Experiments were performed on single stage gas guns. Samples of the aluminium alloy 7010-T6 were cut from a single hot rolled block. As a consequence of the hot working process the material has a characteristic pan-cake grain structure (with the long axis of the grains in the rolling direction), which shows dynamic recovery but not dynamic recrystallisation. Manganin stress gauges (MicroMeasurements LM-SS-125CH-048) were supported on the back of the alloy targets with 12 mm blocks of polymethylmethacrylate (PMMA). Calibration studies by Rosenberg *et al* [8] were used to convert voltage-time data from the gauges into stress–time. Specimen configuration and gauge placement is shown in Figure 1.

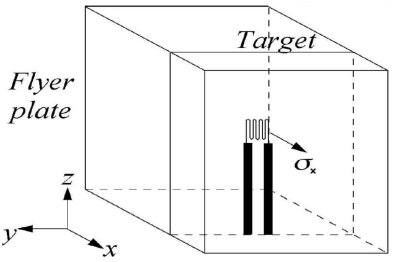

Figure 1 - Specimen configuration and gauge placement.

A dural (aluminium alloy 6082-T6) flyer was chosen as an impactor since it had a close similarity in acoustic properties to the target. The geometry of the target and the impactor was chosen so that the reflected complete releases from target and flyer would interact in the centre of the 7010 target plate. Impact velocities were chosen to be around twice and three times the HEL of the material, that is *ca*. 450 m s^{-1} and 895 m s^{-1}. A test at the lower velocity of 234 m s^{-1} was also performed.

Hydrocode Modelling

The main purpose of the modelling studies was firstly to compare the performance of explicit finite element codes and smoothed particle hydrodynamics (SPH) codes, secondly to investigate the capability of current constitutive models to accurately predict the material behaviour under high velocity impacts. Thirdly, to obtain an insight into some of the experimental observations and attempt to explain their physical significance. It was clear that some of these observations challenged quite long-standing views of the physics of spallation. Modelling therefore provided a potentially powerful and independent approach to investigating the issues. The main reason for this is that hydrocodes do not make any pre-determined assumptions concerning the stress-system or wave propagation behaviour. They solve the conservation equations and use the constitutive models and equations of state to determine dynamic the material response.

The simulations of these tests were performed using the public domain version of the Lagrangian hydrocode DYNA3D originating from Lawrence Livermore National Laboratory, and an in-house developed SPH code. The Al7010 plate was characterised using an anisotropic plastic-hydrodynamic material model that was developed at Cranfield University. The model uses Hill's anisotropic yield criterion [4]:

$$f(\sigma_{ij}) = \left[F(\sigma_y - \sigma_z)^2 + G(\sigma_z - \sigma_x)^2 + H(\sigma_x - \sigma_y)^2 + 2L\sigma_{yz}^2 + 2M\sigma_{zx}^2 + 2N\sigma_{xy}^2\right]^{\frac{1}{2}} - \sigma_{yield} = 0 \quad , \qquad (1)$$

and has a strain rate dependent yield stress and hardening modulus. The constitutive equations are integrated using the tangent stiffness method. The spherical part of the stress tensor is calculated using an equation of state. A Grüneisen equation of state was used in all presented results. In order to model the spallation, which is clearly observed in the experimental results, a principal stress based spall criterion was used. This criterion detects spall if the maximum principal stress exceed a specified limit.

The characteristic of this plate impact problem is that it can be reduced to a 1-D wave propagation. Hence building an model is greatly simplified. The model that was used for this simulation the three materials where modelled as rectangular bars. Symmetry planes where applied on all the sides. This will result in a 1D wave travelling along the length of the bar. The stress time histories where recorded in the elements at the back of the test specimen. A non-reflecting boundary condition was applied at the back of the PMMA block. This will ensure that no release wave travels back through the PMMA in to the AA7010-T6 block as this would unload the test specimen. The impactor is modelled with 25 elements along the axis of impact, the test specimen and the PMMA block are modelled with 75 and 100 elements along the axis of impact respectively (Fig. 2). A contact interface was specified between the impactor and the test specimen. The stress time histories

where recorded in the elements at the back of the test specimen. These mesh resolutions were sufficient to allow the resolution of all the relevant elastic and plastic waves in the target and flyer. The SPH simulation was performed as a one dimensional simulation. In total 458 particles were used to model the three materials. Again, a contact interface was applied between the target and impactor. This was achieved using a penalty stiffness algorithm.

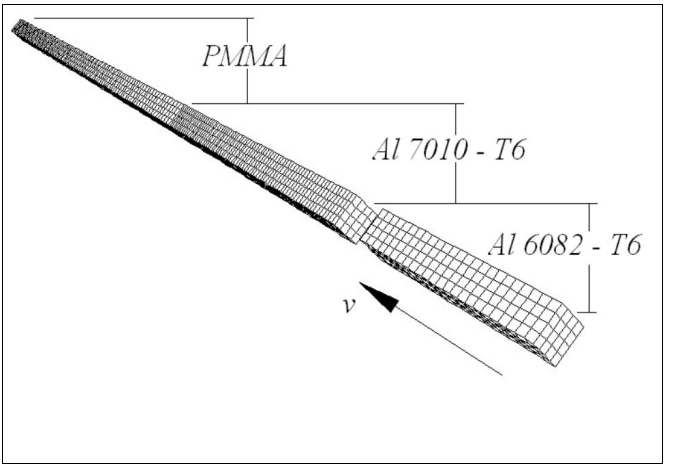

Figure 2 – FE Mesh

The three impacts where simulated with a principal stress based spall criterion. This spall model detects spall when the maximum principal stress respectively reaches a certain limit, and then sets the stresses to zero and does not allow any tensile hydrostatic stress.

Results and Discussion

In Figures 3 to 8 the experimetal and simulation results are presented. The experimetal results are plotted on each graph to allow for comparison. The general shape of the stress traces compares very well with the experiments for both FE and SPH simulations. In the SPH simulation results show a slight overestimation of the wave propagation speed. One can clearly see the different HEL's that are obtained when the material is impacted in different directions demonstrates that the anisotropic plasticity model is adequate (Fig. 3 to 6). Furthermore the good agreement of the general pulse shape and Hugoniot stress level show that the Equation of State (EoS) is performing satisfactorily. All results are summarised in Table 1.

In Figures 3 and 4 the results for the 234 m/s impact are presented. No spall occurs at this impact velocity, so the characteristic pull back signals are not present. The results obtained with the SPH code are ver similar to the finite element results. Both show good general agreement with the experimental results. The difference in

the HEL is clearly present in both simulations. The FE results are in reasonable agreement with the experiment and predict values of 0.43 and 0.39 GPa, in the rolling and transverse directions respectively, compared to 0.39 and 0.33 GPa in the experiment. The SPH simulation predicts 0.36 and 0.33 GPa, which is in better agreement than the FE results. The Hugoniot stress levels are in very good agreement with the experiment with both the FE and SPH simulations prediciting a level of 0.63 compared to 0.65 GPa measured in the experiment.

In Figures 5 and 6 the simulated gauge traces at the higher impact velocity of 450m s^{-1} (at two times the HEL) are presented in which clear spall signals are resolved. Again one can observe a difference in HEL, depending on the direction of impact. The Hugoniot stress levels are 1.28 GPa (FE) and 1.30 GPa (SPH) for the simulation and 1.3 and 1.4 GPa, depending on direction of impact, in the experiment. Again, this is in very good agreement. One can clearly see pull back signals in both traces which indicate spall. The measured values of the pull back signal (spall) in the experiment at 450 m s^{-1} are 0.31 GPa in the longitudinal orientation and 0.45 GPa in the short transverse. The values of the pull back signal in the simulation using the principal stress criterion are not really affected by the direction of impact, and are around 0.2 GPa (FE) and 0.28GPa (SPH) for both directions It is clear that the current simple spall models are inadequate to qualitatively model spall behaviour.

At the 895 m s^{-1} impacts the picture is similar. The general shape of the pulse agrees quite well with the experiment (see Figures 7 and 8), the Hugoniot stresses also compare well. In the experiment values of 3.25 GPa in the longitudinal direction and 2.8 GPa in the transverse direction are recorded. The simulation results predict a value of 2.9 GPa (FE) and 2.93 GPa (SPH). For the comparison of the spall signals the situation again similar to the 450 m s^{-1} impact. In the simulation the pull back signals are 0.15 GPa (FE) and 0.18 GPa (SPH), while the experiments record 0.37 GPa in the longitudinal orientation and 0.18 GPa in the short transverse. The main point here is that the pull back signals here compare reasonably well with the experimentally recorded one in the transverse direction. With the simple spall models that are being used one can not expect to observe the complex evolution of spall strength with a change stress levels and strain rates. These trends can not be explained by first order spall theory, and further work is required to understand this process.

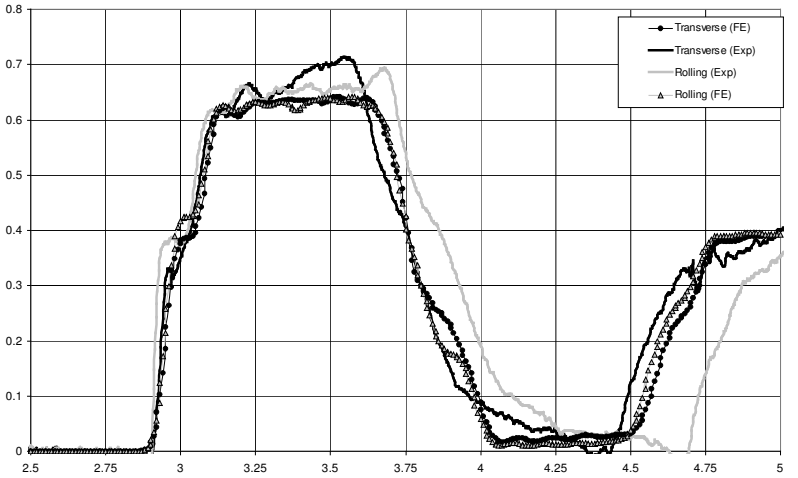

Figure 3 - 234ms FE

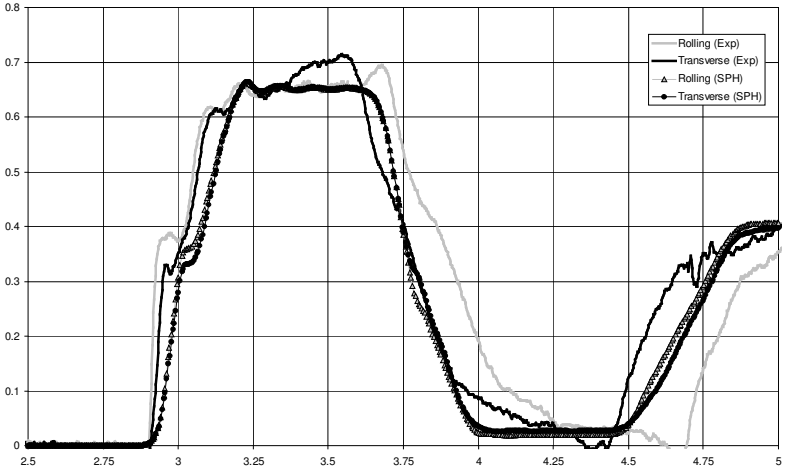

Figure 4 - 234ms SPH

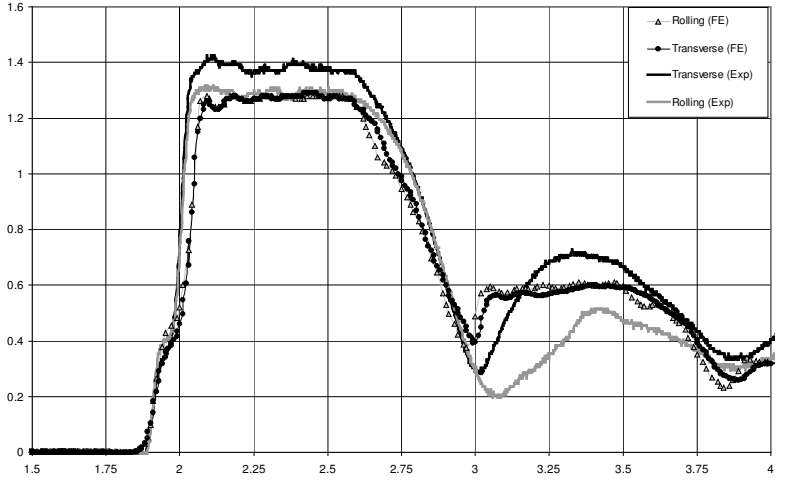

Figure 5 - 450ms FE

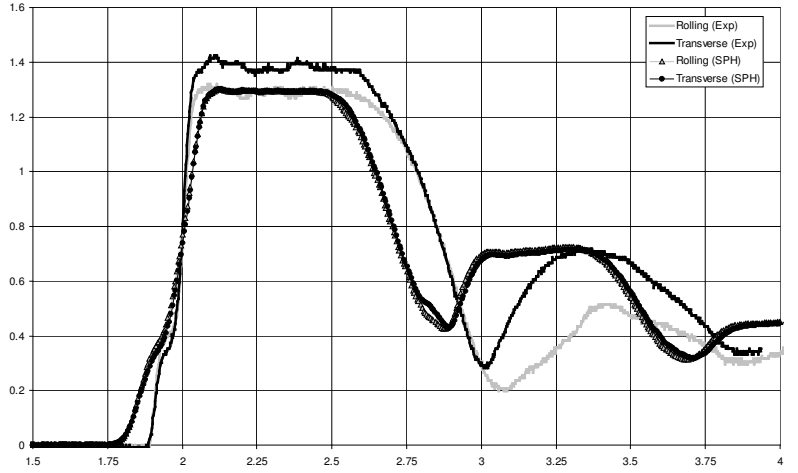

Figure 6 - 450ms SPH

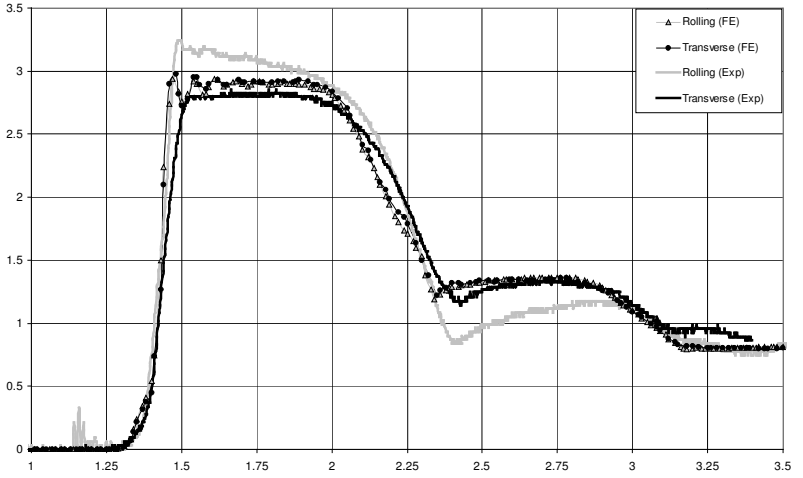

Figure 7 - 895ms FE

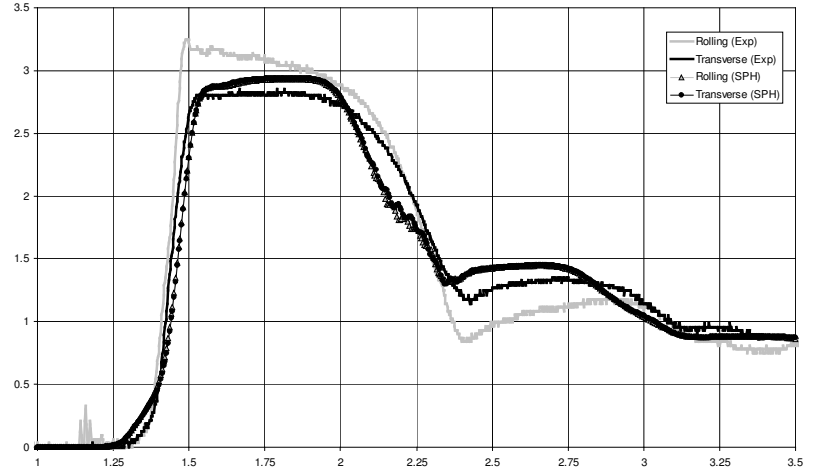

Figure 8 - 895ms SPH

The main conclusion one can draw from these 1D SPH simulation results is that the SPH method has the potential performs as good as finite element analysis in simulating this type of wave propagation and failure in anisotropic solids. If the simulation results of a 3D SPH simulation can match the results obtained of the 1D simulation then the SPH method could be a more powerful tool in testing new material models than conventional FE methods. The reasons for this are that it is easier to implement new material models and the fact that it is much easier to model failure or crack formation and propagation in SPH.

Vel.	Variable	Rolling			Transverse		
		Exp	FE	SPH	Exp	FE	SPH
234 [m/s]	HEL [GPa]	0.39	0.43	0.36	0.33	0.39	0.33
	Hugoniot Stress [GPa]	0.65	0.63	0.65	0.65	0.63	0.65
	Spall Strength [GPa]	N/A	N/A	N/A	N/A	N/A	N/A
450 [m/s]	HEL [GPa]	0.39	0.43	0.38	0.33	0.39	0.35
	Hugoniot Stress [GPa]	1.30	1.28	1.30	1.40	1.28	1.30
	Spall Strength [GPa]	0.31	0.20	0.28	0.45	0.20	0.28
895 [m/s]	HEL [GPa]	N/A	N/A	N/A	N/A	N/A	N/A
	Hugoniot Stress [GPa]	3.25	2.90	2.93	2.80	2.90	2.93
	Spall Strength [GPa]	0.37	0.15	0.15	0.18	0.15	0.15

Table 1 - Summary of Results

The simple spall model that has been used is capable of predicting whether or not spall occurs. But it is not capable of accurately simulating the pull back signals that result from spall. In order to be able to simulate these signal accurately further work is required in the development of spall models, especially if one is to simulate the complex spall behaviour observed in Al 7010 – T6, where the spall strength increases with strain rate, but reduces with stress levels. This will require further work both on the experimental and constitutive modelling level.

Conclusions

FE and SPH plate impact simulations have been performed on the aluminium alloy 7010, in the peak-aged condition, where the HEL and spall strength have been compared with the experimental results. This demonstrated the ability of the SPH method to be used as a simulation tool for this kind of wave propagation and material failure problems.

It was found that the current model is capable of simulating the higher HEL in the longitudinal direction compared to the short transverse, following the trends of the quasi-static yield stress. The Hugoniot stress levels are predicted to a high level of accuracy, as well as the general shape of the pulse and pulse width.

The spall model that was tested is able to qualitatively predict spall. However it is not capable of predicting the pull back stress level at any degree of accuracy. If simulation is to be used to better understand the material behaviour under impact loading further work will be required in order to improve the simulation of spallation of the material. More complex spall models are required, which will require further work both on the experimental and constitutive modelling level.

References

[1] D. R. Ek and J. R. Asay, Y. M. Gupta, Eds., *Shock Compression of Condensed Matter 1985*, New York, Plenum, 1986.

[2] G. T. Gray III, N. K. Bourne, M. A. Zocher, P. J. Maudlin, and J. C. F. Millett, and M. D. Furnish, L. C. Chhabildas, and R. S. Hixson, Eds, *Shock Compression of Condensed Matter - 1999*, Woodbury, NY, AIP Press, 2000.

[3] G. T. Gray, M. F. Lopez, N. K. Bourne, J. C. F. Millett, and K. S. Vecchio, and, N.N. Thadhani and Y. Horie, Eds, *Shock Compression of Condensed Matter – 2001*, Woodbury, NY, AIP Press, 2001 (in press).

[4] R. Hill, *The Mathematical Theory of Plasticity*, Oxford, Oxford University Press, 1950.

[5] J. C. F. Millett and N. K. Bourne, The effects of orientation on the strength of the aluminium alloy 7010 – T6 during shock loading, *Scripta Materialia*, Submitted, 2001.

[6] E. Moshe, S. Eliezer, E. Dekel, A. Ludmirsky, Z. Henis, M. Werdiger, N. Eliaz, and D. Eliezer, An increase in the spall strength in aluminium, copper and metglass at strain rates larger than 10^7 s^{-1}, *Journal of Applied Physics*, Vol. 83, pp. 4004-4011, 1998.

[7] Z. Rosenberg, G. Luttwak, Y. Yesherun, and Y. Partom, Spall studies of differently treated 2024A1 specimen, *Journal of Applied Physics*., Vol. 54, pp. 2147-2152, 1983.

[8] Z. Rosenberg, D. Yaziv, and Y. Partom, Calibration of foil-like manganin gauges in planar shock wave experiments, *Journal of Applied Physics*. Vol. 51, pp. 3702-3705, 1980.

[9] R. E. Smallman, *Modern Physical Metallurgy*, 4th ed., London, Butterworths, 1985.

[10] J. Zheng and Z.-P. Wang, Spall Damage in Aluminium Alloy, *International Journal of Solids and Structures*, Vol. 32, pp. 1135-1144, 1995.